Progress In Electromagnetics Research, PIER 28, 1–16, 2000

ELECTROMAGNETIC EFFECTS ASSOCIATED WITH A CAVITY-BACKED APERTURE LOADED WITH NONLINEAR ELEMENTS

Z. Wu and R. W. Ziolkowski

Department of Electrical and Computer Engineering
The University of Arizona
Tucson, AZ 85721, USA

1. INTRODUCTION

A prominent problem encountered in a variety of EMC and RCS studies is the prediction of the amount that an electromagnetic wave will penetrate through an aperture into a cavity and the level of the subsequent interaction that the coupled wave energy will have with elements within the cavity. This aperture penetration problem has been encountered in many studies of the interactions of high power microwaves with targets such as aircraft and missiles. While the coupled energy effects are concentrated primarily upon front-door (direct paths, e.g., coupling

directly through a radar antenna) mechanisms, it has been recognized that back-door effects (indirect paths, e.g., coupling through apertures or holes in conducting surfaces such as seams in a fuselage) also play a major role in allowing energy into a cavity. A system may be vulnerable if significant levels of microwave energy reaches a particular component.

On the other hand, the EMC and RCS communities must deal with the reciprocal of these shielding problems. The RCS problem concentrates on the issue of how much energy is scattered back into the far field by these cavity-backed apertures. The scattering by fan blades behind an engine cowling is now a classic example of this issue. The EMC problem associated with emission standards must deal with how much energy can escape into the far field from a device contained within a shielded enclosure. A basic understanding of the coupling processes has been established with a number of canonical structures, e.g., infinite conducting cylinders with infinite axial slots with interior loadings as investigated by many researchers, for instance, [1–11], spheres with circular holes, for instance, [12–14], and rectangular cavities with slots, for instance, [15, 16]. In particular, it has been demonstrated theoretically, numerically, and experimentally that the backscattered data from a cavity-backed aperture contains significant information about the interior of the cavity at frequencies corresponding to its natural resonances. Moreover, if the cavity is loaded, the properties of the loads impact this backscattered data significantly. The loads considered in these canonical examples were primarily bulk objects that were concentric with the open cavity or were simple wire antennas with no loads that acted as measurement probes. The determination of the RCS or EMC effects when the load in the interior region of the cavity is complex has received little attention.

In this paper we concentrate on the variations of the field penetration into the cavity and the field scattered from the cavity-backed aperture when nonlinearly-loaded antennas are present in the interior region of the cavity. We determine the difference in the field values both inside and outside of the cavity between the case in which there is nothing inside the cavity and the case in which there is one or a set of diode loaded, dipole antennas present. The dipole antenna model is adopted here as it is a well known fact that the wiring on a printed wiring board(PWB) can be fairly well represented by a dipole antenna over a wide frequency range. Additionally, most interior systems con-

tain some form of nonlinearity such as an oscillator or an amplifier so the issue of determining what nonlinear effects exist is a reasonable one. We will focus attention on the simplest nonlinear element—the diode. If significant effects are not produced or are inexplicable with a diode load, then dealing with more complex systems will be hopeless.

Because the load of the dipole antenna is assumed to be nonlinear, the behavior of the interaction between a broad bandwidth incident signal and the cavity-backed aperture with an enclosed nonlinearly-loaded dipole antenna can not be realized from a frequency domain analysis. A transient analysis is necessary. A full wave, vector FDTD characterization is emphasized throughout this paper. The modeling of the interaction of an electromagnetic field with the nonlinearly-loaded dipole antenna is accomplished with extensions of the FDTD simulator to include the additional governing ordinary differential equation(ODE) that models the circuit voltage and current of the load. The FDTD extension is provided by the nonlinear diode modeling associated with the artificial material studies given in [17]. This approach incorporates the nonlinear diode model directly into the update equation set. More complex loads can be treated readily with a combined FDTD-SPICE solver. It will be demonstrated that even for the simple diode load, frequency responses in the interior and backscattered fields appear at values other than those contained in the incident waveform because of the presence of the nonlinear elements. In addition, it is shown that, as in the linear cases, those responses are dominated by the resonance features corresponding to the open, loaded cavity.

2. NONLINEARLY LOADED DIPOLE ANTENNA MODEL

The antenna enclosed within the cavity will be assumed to be electrically small. This is a reasonable assumption if we consider, for example, an antenna that corresponds to a trace between components on a circuit board enclosed within the cavity. Moreover, it allows us to model the antenna and its load within one cell of the FDTD simulation space. Then one only needs to specify the models of the antenna and of its load to integrate effectively the entire element into the FDTD simulator.

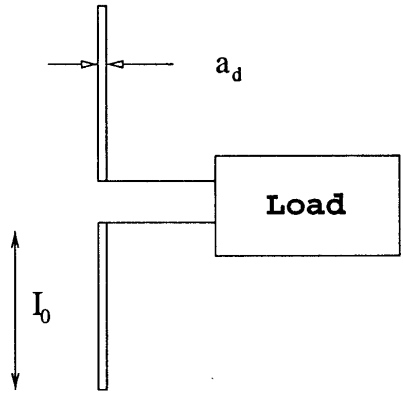

Figure 1. Basic description of the electrically small loaded dipole antenna.

2.1 Antenna Model

Consider the electrically-small loaded, dipole antenna shown in Fig. 1, which has the half-length l_0 and wire diameter a_d. The current i at its terminals is related to the interacting electric field through the relations [17]:

$$\epsilon_0 \frac{\partial}{\partial t}\vec{E} = \nabla \times \vec{H} - \frac{\partial}{\partial t}\vec{P} \tag{1}$$

$$\mu_0 \frac{\partial}{\partial t}\vec{H} = -\nabla \times \vec{E} \tag{2}$$

$$\frac{\partial}{\partial t}\vec{P} = -\frac{l_0}{V} i\vec{n} \tag{3}$$

where $\vec{P}$ is the effective polarization of the dipole and $\vec{n}$ is unit vector which represents its orientation. The constant V represents the effective volume associated with the dipole. Here it is chosen to be 20 times as large as the physical volume of the antenna, i.e.,

$$V = 20.0 \times \left[\pi \left(\frac{a_d}{2}\right)^2 (2l_0)\right] \tag{4}$$

so that the effective volume is slightly more than the volume of a cube whose side has a length equal to the size of the antenna when the radius of the wire is taken to be a tenth of its length, i.e., if $a_d = 0.1 \times (2l_0)$,

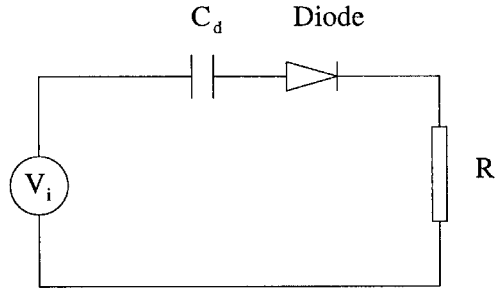

Figure 2. Equivalent circuit of the dipole antenna and its load.

then $V = 1.26 l_0^3$. The source voltage for the circuit is given by the open circuit voltage of the antenna with no load:

$$v_i = -l_0 \vec{E} \cdot \vec{n} \tag{5}$$

Because the current established in the dipole antenna is very dependent on its load, the operating characteristics of that load will determine the response of the resulting wave interactions with the antenna.

2.2 Diode Model

The diode is one of the simplest and best characterized passive nonlinear devices that is commonly found in many circuits. It is generally modeled by the nonlinear current-voltage expression:

$$i(t) = I_s \left(e^{\alpha v_d(t)} - 1 \right) \tag{6}$$

For our study we set the constant α to the value of $40.0 V^{-1}$ and the amplitude constant I_s to the value $6.0 \times 10^{-8} A$.

2.3 Formulation of the Extended FDTD Update Equations

When the load attached to the dipole antenna consists of the diode and a small resistor, it may be represented by an equivalent Thevenin circuit as shown in Fig. 2. The constant $C_d = \pi \epsilon_0 l_0 / ln(4.0 l_0 / a_d)$ is the equivalent capacitance of the electrically small dipole antenna. After applying some basic circuit analysis techniques and taking into account the effects of the nonlinear diode model Eq. (6), the following

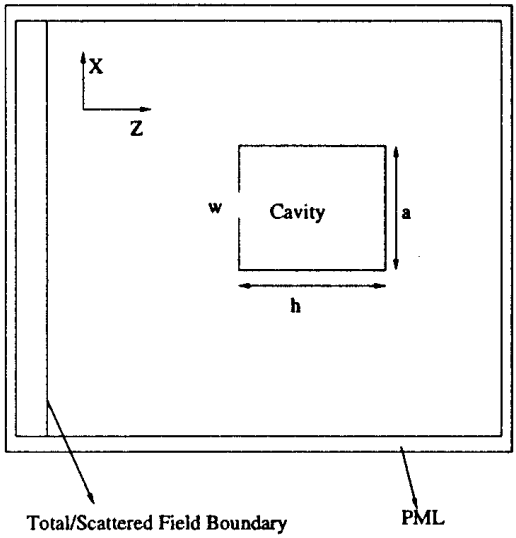

Figure 3. Cross sectional view of the computional region (infinite in the y direction), rectangular PEC cavity of side a, height h and aperture size w.

differential equation is generated which describes the behavior of the dipole and its nonlinear load [17]:

$$\frac{di}{dt} = \frac{\alpha(i + I_s)}{1 + R\alpha(i + I_s)} \left(\frac{dv_i}{dt} - \frac{i}{C_d} \right) \tag{7}$$

As shown below and in [17], Eq. (7) can be combined with Eqs. 1–3 in a standard FDTD simulator to model the behavior arising from the nonlinearly-loaded dipole antenna.

3. EXTENDED FDTD UPDATE EQUATIONS

A skematic of the FDTD computional region is given in Fig. 3. Square cells are used to construct the FDTD grid. A plane wave is launched from a total field-scattered field boundary to illuminate the cavity. The plane wave is assumed to be normally incident on the cavity to simplify the analysis and to maximize the coupling into the interior of the cavity. The simulation region is terminated with a 10-cell thick, quadratic PML layer optimized for the frequency region of interest.

3.1 TM Case

As noted previously, the dipole antenna is assumed to be contained within one FDTD cell. If the dipole is assumed to be oriented in the x-direction, then $\partial P_x/\partial t = -(l_0/V)i$ so that Eqs. (1), (2), and (3) lead to the following expressions:

$$\epsilon_0 \frac{\partial}{\partial t} E_x = -\frac{\partial}{\partial z} H_y + \frac{l_0}{V} i \tag{8}$$

$$\epsilon_0 \frac{\partial}{\partial t} E_z = \frac{\partial}{\partial x} H_y \tag{9}$$

$$\mu_0 \frac{\partial}{\partial t} H_y = \frac{\partial}{\partial x} E_z - \frac{\partial}{\partial z} E_x \tag{10}$$

Combining this system with Eqs. (5) and (7), one finds that the current of the diode is related to the magnetic field H_y by the relation:

$$\frac{di}{dt} = \frac{\alpha(i + I_s)}{1 + R\alpha(i + I_s)} \left(\frac{l_0}{\epsilon_0} \frac{\partial H_y}{\partial z} - \left(\frac{1}{C_d} + \frac{l_0^2}{\epsilon_0 V} \right) i \right] \tag{11}$$

Consequently, the final extended FDTD update equations for the TM case consist of finite difference versions of Eqs. (8), (9), (10), and (11). The electric field is obtained at integer time steps while the magnetic field is obtained at half-integer time steps. A Runge-Kutta integrator is used to solve the nonlinear Eq. (11) for the current at each integer time step.

3.2 TE Case

The extended FDTD update equations for the TE case follow in an analogous manner to those obtained for the TM case. We thus include here only the final continuum equations for the TE case. Note that the dipole antenna will interact effectively with the wave in this case only if the dipole is oriented in the y direction. The extended equation set that is used to achieve the update equations for the FDTD simulations of the TE cases is:

$$\frac{di}{dt} = \frac{\alpha(i + I_s)}{1 + R\alpha(i + I_s)} \left[\frac{l_0}{\epsilon_0} \left(\frac{\partial H_z}{\partial x} - \frac{\partial H_x}{\partial z} \right) - \left(\frac{1}{C_d} + \frac{l_0^2}{\epsilon_0 V} \right) i \right] \tag{12}$$

$$\mu_0 \frac{\partial}{\partial t} H_x = \frac{\partial}{\partial z} E_y \tag{13}$$

$$\mu_0 \frac{\partial}{\partial t} H_z = -\frac{\partial}{\partial x} E_y \tag{14}$$

$$\epsilon_0 \frac{\partial}{\partial t} E_y = \frac{\partial}{\partial z} H_x - \frac{\partial}{\partial x} H_z + \frac{l_0}{V} i \tag{15}$$

4. FDTD SIMULATION RESULTS

A variety of TM and TE configurations were tested with the extended FDTD simulator. In addition, several different values of the diode circuit components were simulated. The following summarizes those results.

4.1 TM Case

The open cavity shown in Fig. 3 is 0.7 m in the x direction ($a = 0.7\,\mathrm{m}$) and 1.0 m in the z direction ($h = 1.0\,\mathrm{m}$). The size of the aperture is 0.08 m. The cavity is excited by 20 cycles of a sinusoid wave at 150 MHz. The spectrum of the incident magnetic field is shown in Fig. 4. The simulation is run with a grid consisting of square cells having an edge length of $\lambda/100 = 2.0\,\mathrm{cm}$ at an effective frequency of 150 MHz. Thus the cavity is 35 cells $\times 50$ cells with the aperture occupying 4 cells in the x direction. The half-length of the dipole is set at $l_0 = 1.0\,\mathrm{cm}$ and the wire diameter is selected as $a_d = 0.1\,\mathrm{cm}$. The dipole thus fits inside one of the FDTD cells; the relatively low incident frequency choice allows the desired treatment of the dipole antenna as a lumped element inside one FDTD cell. The value of the series resistor is fixed at $10\,\Omega$ for all the runs reported below. Our FDTD simulator is run in double precision to minimize the numerical inaccuracies.

The incident pulse launched at the open cavity and the resulting scattered fields are followed by the simulator for 20,000 time steps. This guarantees that there will be sufficient time for the pulse to interact with the cavity and to set up all possible modal patterns inside it. The magnetic field component H_y is used to quantify the field structures within the simulation region. We consider the case where the incident magnetic field has an amplitude of 3.0 A/m to fully explore whatever nonlinear effects might be associated with this nonlinearly-loaded open cavity.

As noted in Sec. 1, the resonance features corresponding to the presence of the interior cavity dominate the aperture coupling and the

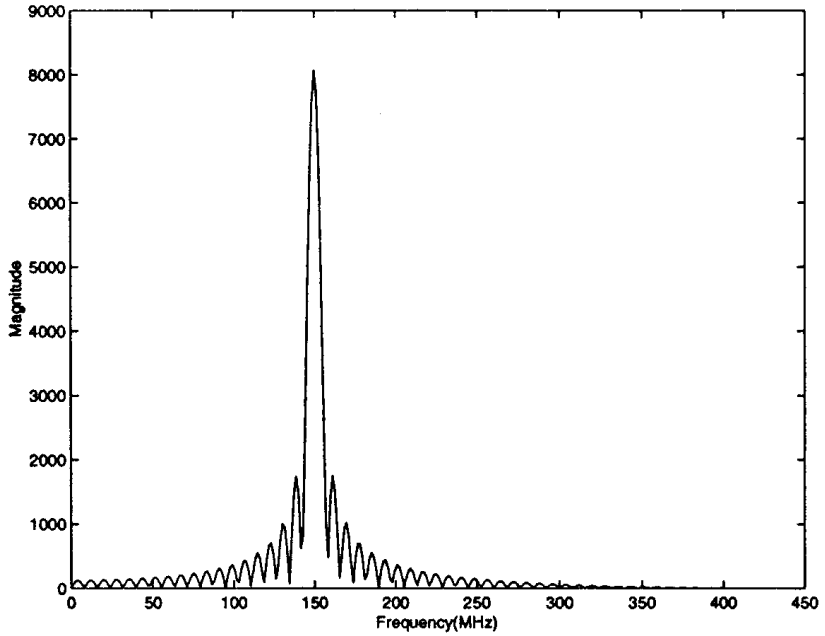

Figure 4. Spectral of the incident magnetic field.

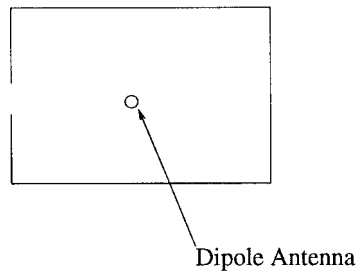

Figure 5. Cavity configuration 1.

scattering results. These resonances also are dependent on the characteristics of the interior load. We are interested in how the arrangement of the nonlinearly-loaded dipole antennas inside the cavity affects the modal patterns that will be established in the interior of cavity; and, furthermore, how the fields sensed in the far field are correlated to these changes in the modal patterns. Because only a few of the cells

inside the cavity will contain nonlinearly-loaded dipole antennas, we don't expect the magnitude of the nonlinear effect associated with their presence to be very large when compared to the coupled and scattered fields associated with the corresponding empty cavity case. Consequently, instead of investigating the absolute field values, we focus attention on the change of the field values inside the cavity and in the far field that are caused by the presence of the nonlinearly-loaded dipole antennas. The simulation approach is thus to run the FDTD simulator two times: the first time only with an empty open cavity and the second time with our desired placement of the nonlinearly-loaded dipoles in the same cavity. In this manner the subtraction of the fields obtained from both cases can be made in the frequency domain to determine the spectrum of the additional effects both in the interior and the exterior of the open cavity due to the presence of the nonlinear elements.

In particular, we proceeded by selecting three random sampling points in the interior of the cavity, an observation point just inside the cavity near the aperture, and an observation point in the backscattered far field region. With these probe points we were able to obtain time histories which characterized the interaction of the incident wave with the unloaded and the nonlinearly-loaded structure. After Fourier transformation, the resulting spectrum gave us detailed information about the modal pattern set up inside cavity, around the aperture and in the far field respectively for those cases.

Consider first the cavity configuration depicted in Fig. 5. One dipole antenna is located at the center of the cavity. The aperture is set at the center of the source side of the cavity. The modes of the closed cavity that appear below 600 MHz are TM_{10}, TM_{11}, TM_{20}, TM_{21}, TM_{30}, TM_{12}, and TM_{22}, and they appear, respectively, at the frequencies 150.00 MHz, 261.57 MHz, 300.00 MHz, 368.67 MHz, 450.00 MHz, 454.06 MHz, and 523.14 MHz. Thus, the incident field can excite the lowest order cavity mode; and the higher harmonics, which can be generated by the diode, coincide with several frequencies that correspond to the higher order cavity modes. The spectra of the differences of the field strengths between the unloaded and the loaded open cavity cases at the various sample locations are shown in Fig. 6. Note that frequencies other than the incident one have been generated, and the magnitude of the exterior response is on the order of 10^{-3} of that of incident field while the interior response is an order of magnitude

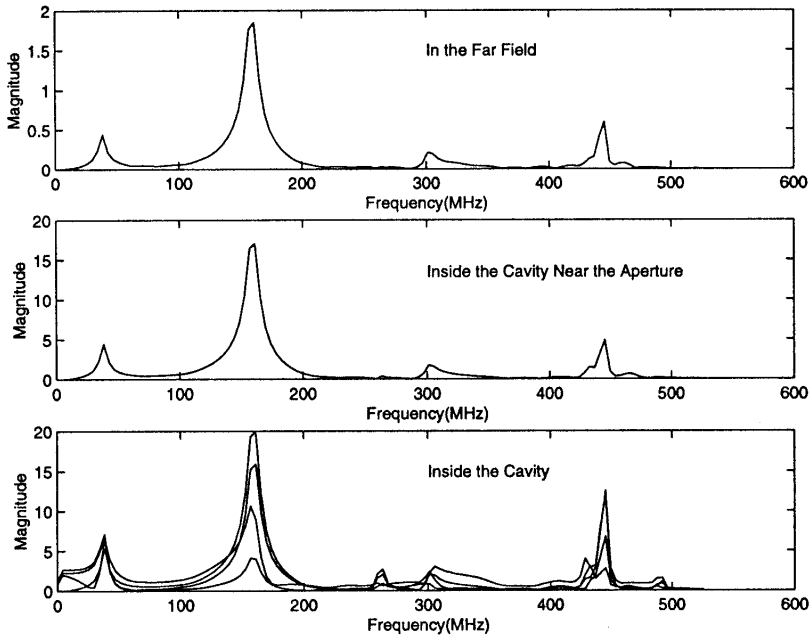

Figure 6. Magnetic field spectrum of config. 1.

larger than these exterior values. Fig. 6 also shows that the nonlinear response of the loaded cavity is highly correlated with the unloaded cavity's resonance features, the locations of which in the frequency domain are well identified by the corresponding closed-cavity resonance locations because of the small size of the aperture. Note that the current element of the dipole antenna could be physically treated as an electric current probe which serves as a feedline that, due to its nonlinear current characteristics, would couple energy to those modes that have non-zero electric field distribution at the position of the dipole. In other words, some modes inside the cavity could be selectively excited to the exclusion of other modes. In fact, in the cavity config. 1, the TM_{10}, TM_{30}, TM_{12}, and TM_{11} modes inside cavity are enhanced as compared to the case of the same empty cavity, because the location of the dipole antenna corresponds to the peak value of these modes' transverse electric field. In comparison, the TM_{20} and TM_{21} modes are suppressed since their electric fields have nulls where the dipole antenna is located. Also note that the first resonance in the far field response is attributed to the capacitance of the aperture. This phe-

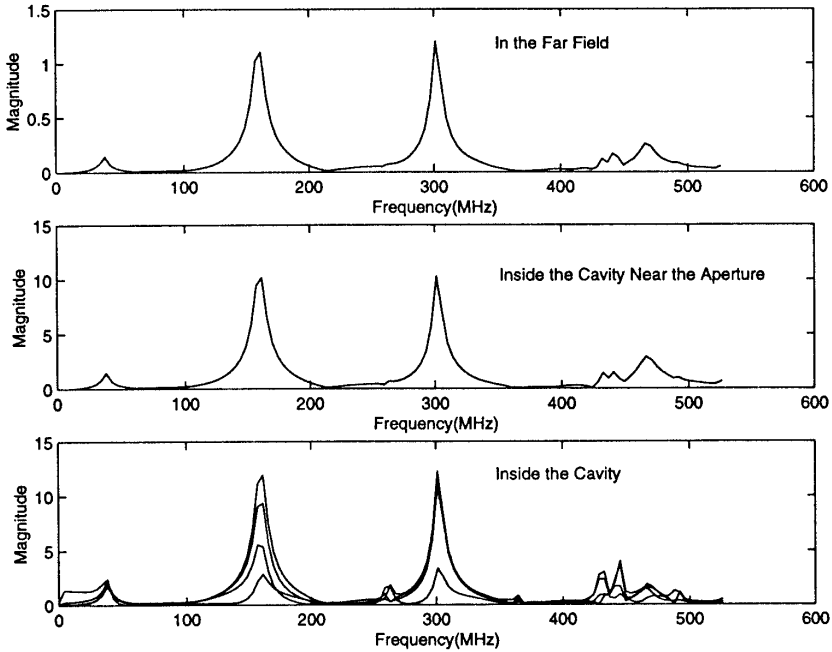

Figure 7. Magnetic field spectrum of config. 2.

nomena has been reported previously in [11], and it is associated with the discontinuity of the induced current across the aperture.

To further verify these observations, in cavity config. 2 the dipole antenna was moved a distance $3h/4$ away from the aperture to the location where the TM_{20} and TM_{21} modes were expected have their peak values. The result is shown in Fig. 7. Clearly it is confirmed that the TM_{20} and TM_{21} modes are now enhanced in contrast to the case of config. 1. The TM_{10} mode in both cases displays a relatively strong resonance because it is the dominant mode of the cavity and there exists no null of the corresponding electric field distribution inside the cavity except on two walls.

We further note that not all the modes established inside cavity could be detected in the far field. The far field response depends on the specific modal pattern exhibited around the aperture, i.e., if the peak of a mode is situated at the aperture, then this mode will have maximum reradiation or coupling to the far field. On the contrary, if the node of a mode occurs near the aperture, minimum radiation effects will occur. To test this, we ran cavity config. 3 which was the

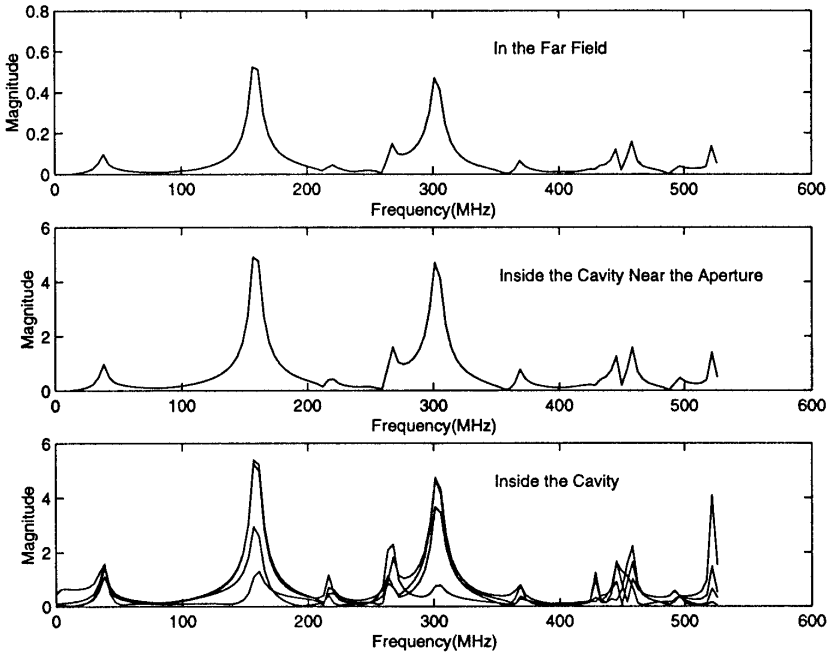

Figure 8. Magnetic field spectrum of config. 3.

same as cavity config. 2 except that the aperture was moved 8 cm off-center. The results shown in Fig. 8 demonstrate that the spectra observed in the far field have the same distinctive resonance features as they appear inside the cavity. The offset of the aperture allows nearly all the modes generated by the dipoles to couple to the fields outside of the cavity.

Cases were also run in which multiple dipole antennas were placed inside the cavity. The results proved to be consistent with what was obtained with single dipole. Accumulative effects were observed both inside the cavity and in the far field, i.e., for N dipoles, the resonant magnitude was N times larger than for the single dipole case. However, note that because the dipoles were physically separated by several cells, there were no significant direct nonlinear interactions between the nonlinearly-loaded dipole antennas themselves. We simply found that if an antenna was placed at a maximum of the mode, then its response contributed significantly to the interior and exterior response of the open cavity. Thus, as long as the dipole antennas were not arranged

very near to each other, the results did not manifest strong linear or nonlinear couplings among the dipoles.

4.2 TE Case

The TE polarization cases were also run and compared with the TM polarization results. We found that the physical phenomena related to the nonlinearity and to the cavity's resonance features, which were observed in the TM polarization case, also applied to the TE polarization cases. However, the field strength in the TE case that is generated by the nonlinearity in the far field is on the order of 10^{-4} of that of the incident field, i.e., a tenth of the value observed in the TM case. This is well explained by the relatively small aperture coupling effect for this polarization. The TE electric field is tangential to the edge of the aperture, hence the field strengths near the edges are small in contrast to the singular edge fields that exist in the TM case. Consequently, we do not explicitly include here any of the TE results.

5. CONCLUSIONS

FDTD studies of cavity-backed apertures enclosing nonlinearly-loaded antennas extend our understanding of the aperture coupling and scattering processes. The interactions of the modal fields corresponding to the resonance features of the cavity with antennas that can nonlinearly generate fields at harmonic frequencies that coincide with those cavity modes lead to extremely interesting interior and exterior responses. The fields sensed in the far field indicate that the exterior scattering data contains information about the nonlinear elements enclosed in the interior of the cavity. This property may have some important applications for object diagnostic and identification purposes.

Only a simple antenna load consisting of a diode and a resistor was treated here. This load was sufficient to demonstrate the generation of harmonic frequencies in the interior and exterior regions of the open cavity. With a more general FDTD-SPICE simulator one could simulate the effects of antennas having more complicated loads. Such configurations are currently under investigation for their EMC and RCS applications; these results will be reported elsewhere.

ACKNOWLEDGMENT

This work was sponsored in part by the Air Force Office of Scientific Research, Air Force Materiel Command, USAF, under grant number F49620-96-1-0039. The U.S. Government is authorized to reproduce and distribute reprints for Governmental purposes notwithstanding any copyright notation thereon. The views and conclusions contained herein are those of the author and should not be interpreted as necessarily representing the Air Force Office of Scientific Research or the US Government.

REFERENCES

1. Butler, C. M., Y. Rahmat-Samii, and R. Mittra, "Electromagnetic penetration through apertures in conducting surfaces," *IEEE Trans. Antennas Propagat.,* Vol. AP-26, 82–93, January 1978.
2. Shumpert, J. D., and C. M. Butler, "Penetration through slots in conducting cylinders - Part 1: TE case," *IEEE Trans. Antennas Propagat.,* Vol. AP-46, 1612–1621, November 1998.
3. Shumpert, J. D., and C. M. Butler, "Penetration through slots in conducting cylinders - Part 1: TM case," *IEEE Trans. Antennas Propagat.,* Vol. AP-46, 1622–1628, November 1998.
4. Mautz, J. R., and R. F. Harrington, "Electromagnetic penetration into a conducting circular cylinder through a narrow slot, TM case," *J. Electromagn. Waves Applicat.,* Vol. 2, 269–293, Mar./Apr. 1988.
5. Mautz, J. R., and R. F. Harrington, "Electromagnetic penetration into a conducting circular cylinder through a narrow slot, TE case," *J. Electromagn. Waves Applicat.,* Vol. 3, 307–336, April 1989.
6. El-Hajj, A., K. Y. Kabalan, and R. F. Harrington, "Characteristic modes of a slot in a conducting cylinder and their use for penetration and scattering, TE case," *IEEE Trans. Antennas Propagat.,* Vol. AP-40, 156–161, February 1992.
7. Colak, D., A. I. Nosich, and A. Altintas, "RCS study of cylindrical cavity-backed apertures with outer or inner material coating: the case of E-polarization," *IEEE Trans. Antennas Propagat.,* Vol. AP-41, 1551–1559, November 1993.
8. Colak, D., A. I. Nosich, and A. Altintas, "RCS study of cylindrical cavity-backed apertures with outer or inner material coating: the case of H-polarization," *IEEE Trans. Antennas Propagat.,* Vol. AP-43, 440–447, May 1995.

9. Johnson, W. A., and R. W. Ziolkowski, "The scattering of an H-polarized plane wave from an axially slotted infinite cylinder: A dual series approach," *Radio Sci.,* Vol. 19, 275–291, Jan./Feb. 1984.
10. Ziolkowski, R. W., W. A. Johnson, and K. F. Casey, "Applications of Riemann-Hilbert problem techniques to electromagnetic coupling through apertures," *Radio Sci.,* Vol. 19, 1425–1431, Nov./Dec. 1984.
11. Ziolkowski, R. W., and J. B. Grant, "Scattering from cavity-backed aperture: The generalized dual serious solution of the concentrically-loaded E-pol slit cylinder problem," *IEEE Trans. Antennas Propagat.,* Vol. AP-35, 504–528, May 1987.
12. Ziolkowski, R. W., and W. A. Johnson, "Electromagnetic scattering of an arbitrary plane wave from a spherical shell with a circular aperture," *J. Math. Phys.,* Vol. 26, 1293–1314, June 1987.
13. Ziolkowski, R. W., "New electromagnetic resonance effects associated with cavity-backed apertures," *Radio Sci.,* Vol. 22, 449–454, July/Aug. 1987.
14. Ziolkowski, R. W., D. P. Marsland, L. Libelo, G. E. Pisane, "Scattering from an open spherical shell having a circular aperture and enclosing a concentric dielectric sphere," *IEEE Trans. Antennas Propagat.,* Vol. AP-36, 985–999, July 1997.
15. Wang, T.-M., and H. Ling, "Resonant behavior of conducting slotted rectangular shells," *Microwave Opt. Tech. Lett.,* Vol. 1, No. 9, 320–323, November 1988.
16. Reed, E. K., and C. M. Butler, "Time-domain electromagnetic penetration through arbitrarily shaped narrow slots in conducting screens," *IEEE Trans. Electromagnetic Compatibility,* Vol. EMC-34, 161–172, August 1992.
17. Auzanneau, F., and R. W. Ziolkowski, "Microwave signal rectification using artificial composite materials composed of diode loaded, electrically small dipole antennas," *IEEE. Irans. Microwave Theory Tech.,* Vol. 46, 1628–1637, November 1998.